Thomas-Fermi model and ferromagnetic phases of magnetic semiconductor quantum dots

Alexander O. Govorov
Department of Physics and Astronomy, Condensed Matter and Surface Science Program, Ohio University, Athens, Ohio 45701-2979, USA
(Received 20 April 2005; published 25 August 2005)

Many-particle electron states in semiconductor quantum dots with carrier-mediated ferromagnetism are studied theoretically within the self-consistent Boltzmann equation formalism. Depending on the conditions, a quantum dot may contain there phases: partially spin-polarized ferromagnetic, fully spin-polarized ferromagnetic, and paramagnetic phases. The physical properties of many-body ferromagnetic confined systems come from the competing carrier-mediated ferromagnetic and Coulomb interactions. The magnetic phases in gated quantum dots with holes can be controlled by the voltage or via optical methods.

DOI: 10.1103/PhysRevB.72.075358 PACS number(s): 73.21.La, 73.21.−b, 73.63.Kv, 78.67.Hc

I. INTRODUCTION

Diluted magnetic semiconductors[1] represent an important class of materials and structures where ferromagnetism can be tuned by voltage.[2] This ability comes from the carrier-mediated character of the ferromagnetic interaction.[3–5] The ferromagnetic ordered state in these systems appears due to mobile carriers interacting with stationary spins of magnetic impurities. To date, Curie temperatures as high as 40 K have been observed in a technologically important class of the Mn-doped III-V semiconductor structures.[6–8] When the magnetic semiconductors become combined with the conventional field-effect layered structures, the number of mobile carriers and the ferromagnetic interaction become tunable by the voltage.[9] This ability to externally control the properties of magnetic crystals with means other than the external magnetic field may have important device applications. A further step from magnetic semiconductor layers would be zero-dimensional systems, quantum dots (QDs). Magnetic quantum dots can be viewed as nanoscale memory elements where information is stored in the form of magnetic polarization. Such a system may have important advantages compared to the conventional metal spin-valve memories: (1) small sizes and relatively small number of carriers and (2) voltage control of the number of electrons which was already demonstrated in many experiments for nonmagnetic QDs.[10,11] Therefore it is important to develop the understanding of magnetic QDs with interacting carriers.

Here we develop a theory of magnetic QDs with many carriers where Coulomb, ferromagnetic, and single-particle energies contribute to the formation of the equilibrium state. Using the quasiclassical description, we show that a QD may be split into three phases with different physical properties. The geometrical sizes of these phases are determined by the Coulomb, ferromagnetic, and single-particle contributions to the chemical potential of a QD. For calculations, we employ the mean-field theory and the Boltzmann kinetic equation. This approach becomes reduced to the Thomas-Fermi model at low temperatures. We should note that our approach ignores the discrete structure of single-particle spectrum of QD and is valid when electrons occupy at least several quantum levels. At the same time, this approach has an important advantage: it allows us to describe the Coulomb effects in relatively large QDs where, as it is shown below, the Coulomb interaction is very strong and significantly exceeds the ferromagnetic interaction and the kinetic energy of carriers. The hole-mediated ferromagnetism in quasi-two-dimensional (2D) systems is strongly anisotropic due to the heavy hole-light hole splitting in the valence band. Therefore, the magnetic polarization occurs predominantly in the growth direction. Then, two magnetic states of a QD with spin polarizations "up" and "down" can represent a single bit.

Presently QDs and other nanostructures doped with magnetic (Mn) impurities attract a lot of attention. Among other studies, several recent theoretical papers investigate QDs and their electron and excitonic states in the presence of a single Mn ion.[12–15] In particular, it was suggested in Ref. 14 that a QD with a single Mn ion can act as a multiqubit which can be controlled optically. Another direction of research describes the magnetic states and polarons in QDs with many Mn ions and one or several carriers.[16–21] Among the above publications, the paper[21] demonstrates that the Coulomb-interaction effects in few-electron QDs can determine a collective magnetic state of holes and Mn spins. Ferromagnetism and spin separation in digital layered structures and quantum wells were also studied in several experimental[6,22] and theoretical publications.[5,23,24]

II. MODEL

As a model system, we are going to use a QD "made out of" a 2D quantum well. Such a zero-dimensional system can be fabricated by etching and lithographical methods. Within the lithographical method, a QD can be defined, for example, by using the top metal gates [Fig. 1(a)]. The number of carriers in such a QD is a voltage tunable parameter.

To describe a state of many carriers confined in a QD, we start from the local properties of the coupled hole-Mn system in a 2D quantum well. In our system, a mobile hole and Mn spins experience an exchange interaction $\hat{U}_{\mathrm{exc}}=-\beta/3\Sigma_i(\hat{S}_{z,i}\hat{j}_z)\,\delta(\mathbf{r}_h-\mathbf{R}_i)$, where β is the exchange interaction constant, and $\hat{S}_z$ and $\hat{j}_z$ are the z components of the spin operators for a Mn spin and hole, respectively; $\mathbf{r}_h$ and $\mathbf{R}_i$ are the coordinates of hole and i impurity, respectively. The

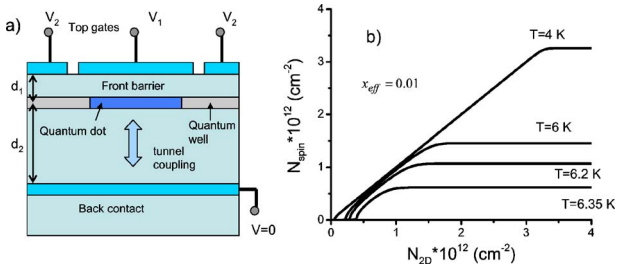

FIG. 1. (Color online) (a) Model of a Mn-doped lithographically defined QD based on a semiconductor quantum well. The number of particles is controlled be the voltage applied between the top and back gates. The QD confinement for holes is given by a voltage difference $\Delta V = V_1 - V_2 < 0$. (b) Calculated 2D spin density as function of the total 2D density of holes at various temperatures; $m_{hh} = 0.38 m_0$, $L = 70$ Å, $N_0 = 23$ nm^{-3}, $\beta N_0 = -2.2$ eV, $x_{\text{eff}} = 0.01$. Curie temperature for the above parameters is about 6.4 K.

above operator describes the interaction between Mn spins and heavy holes and assumes a sufficiently large energy separation between the heavy-hole and light-hole quantized states in the valence band. The corresponding effective spin-dependent potential of a single hole has a form

$$U_{\text{spin}}(j_z) = \frac{j_z}{|j_z|} U^0_{\text{spin}}, \tag{1}$$

where

$$U^0_{\text{spin}}(N_{\text{spin}}) = -\frac{\beta}{3} x_{\text{eff}} N_0 \times \int dz \psi_0^2(z) S_{\text{Mn}} B_{S_{\text{Mn}}}\left[\frac{-\beta}{3}\frac{3}{2} N_{\text{spin}} \psi_0^2(z)\right]. \tag{2}$$

Here $N_{\text{spin}} = N_{+3/2} - N_{-3/2}$ is the net spin 2D density, N_{j_z} are the 2D densities of the spin components, $B_{S_{\text{Mn}}}$ is the Brillouin function, N_0 is the number of cations per unit cell, and $S_{\text{Mn}} = 5/2$. $N_{2\text{D}} = N_{+3/2} + N_{-3/2}$ is the total 2D density in a quantum well. For the ground-state wave function in a quantum well, we will use $\psi_0(z) = \sqrt{2/L} \sin \pi z/L$, where L is the quantum well width. The chemical potential for a 2D gas depends on U^0_{spin} and $N_{2\text{D}}$:

$$\mu_{2\text{D}}(T, N_{2\text{D}}, U_{\text{spin}}) = k_B T \ln\left[-\cosh\left(\frac{U^0_{\text{spin}}}{k_B T}\right) + \sqrt{\cosh\left(\frac{U^0_{\text{spin}}}{k_B T}\right)^2 + \exp\left(\frac{2E_f}{k_B T}\right) - 1}\right], \tag{3}$$

where $E_f(N_{2\text{D}}) = \pi N_{2\text{D}} \hbar^2 / m_{hh}$. Now we calculate the spin polarization

$$N_{\text{spin}} = \frac{k_B T D_{2\text{D}}}{2} \ln\left[\frac{1 + e^{\mu_{2\text{D}} - U^0_{\text{spin}}(N_{\text{spin}})/k_B T}}{1 + e^{\mu_{2\text{D}} + U^0_{\text{spin}}(N_{\text{spin}})/k_B T}}\right], \tag{4}$$

where $D_{2\text{D}} = m_{hh}/(\pi\hbar^2)$. The Zener ferromagnetic phase transition occurs when Eq. (4) has a nonzero solution. Figure 1(b) shows the data for spin density N_{spin} for a GaAs/AlGaAs quantum well with the following parameters: $m_{hh} = 0.38\, m_0$, $L = 70$ Å, $N_0 = 23$ nm^{-3}, $\beta N_0 = -2.2$ eV, $x_{\text{eff}} = 0.01$. The above exchange parameter β is comparable to that used in other publications on magnetic semiconductors (see, e.g., Ref. 23). Since the exchange interaction is antiferromagnetic ($\beta < 0$), the case $N_{\text{spin}} > 0$ corresponds to the negative average polarization of Mn ions, $B_{S_{\text{Mn}}} < 0$. Curie temperature can be analytically calculated in the high-density limit: $k_B T_C = S(S+1)\beta^2 x_{\text{eff}} N_0 m_{hh}/(8\pi\hbar^2)$ ($k_B T_c \ll N_{\text{tot}}/D_{2\text{D}}$).

The in-plane potential in a lateral QD near its center can be approximated by the parabolic function

$$e\phi_0(\mathbf{r}) = U_0 + \frac{m_{hh}\omega^2}{2} r^2, \tag{5}$$

where $e > 0$ is the electron charge and ω is a characteristic frequency of a confining potential. The potential U_0 determines a depth of a lateral potential well. In a QD defined by metal gates [Fig. 1(a)], the parameters U_0 and ω are functions of the gate voltages. In equilibrium, the carrier distribution function, which satisfies the Boltzmann equation, has a form

$$f(p, \mathbf{r}, j_z) = \frac{1}{e^{[p^2/2m_{hh} + e\phi(\mathbf{r}) + U_{\text{spin}}(j_z, \mathbf{r}) - \mu]/k_B T} + 1}, \tag{6}$$

where $\mathbf{r} = (x, y)$ is the lateral position vector and $\mathbf{p}$ is the in-plane momentum. The self-consistent scalar potential of a hole is composed of two terms

$$e\phi(\mathbf{r}) = e\phi_0(\mathbf{r}) + U_{\text{Coul}}(\mathbf{r}), \tag{7}$$

where $U_{\text{Coul}}(\mathbf{r})$ is the electrostatic potential induced by a nonuniform spatial distribution of carriers, $n_{2\text{D}}(\mathbf{r}) = n_{+3/2}(\mathbf{r}) + n_{-3/2}(\mathbf{r})$. In addition, the distribution function (6) depends on the spin of hole through the exchange interaction which is a function of the local spin density $n_{\text{spin}}(\mathbf{r}) = n_{+3/2} - n_{-3/2}$ [see Eqs. (1) and (2)]. At the same time, the function $n_{\text{spin}}(\mathbf{r})$ itself is determined by the total local density of holes $n_{2\text{D}}(\mathbf{r})$ and is given by the numerical solution of Eq. (4) [see the data in Fig. 1(b)]. Therefore, it is convenient to regard U_{spin} as a function of $n_{2\text{D}}$, i.e., $U_{\text{spin}}[j_z, \mathbf{r}] = U_{\text{spin}}[j_z, n_{\text{spin}}(n_{2\text{D}})] = U_{\text{spin}}[j_z, n_{2\text{D}}(\mathbf{r})]$. By integrating the function (6) over momenta we come to two nonlocal nonlinear equations for the densities $n_{\pm 3/2}(\mathbf{r})$. Then, these equations can be solved for the chemical potential and rewritten in the form resembling the central equation of the Thomas-Fermi model:

$$\mu = e\phi_0(\mathbf{r}) + U_{\text{Coul}}(\mathbf{r}) + (j_z/|j_z|) U^0_{\text{spin}}[n_{\text{tot}}(\mathbf{r})] + k_B T \ln[e^{2\pi\hbar^2 n_{j_z}/m_{hh} k_B T} - 1], \quad j_z = \pm 3/2, \tag{8}$$

where $j_z = \pm 3/2$ and $U_{\text{Coul}}(\mathbf{r}) = e^2 \int d^2\mathbf{r}' [n_{2\text{D}}(\mathbf{r})/\epsilon_{\text{eff}}(|\mathbf{r}' - \mathbf{r}|)|\mathbf{r}' - \mathbf{r}|]$, where $\epsilon_{\text{eff}}(\mathbf{r}' - \mathbf{r})|$ is an effective nonlocal dielectric constant of a system with metal gates.[25] We should also note that $U_{\text{Coul}}(\mathbf{r})$ was written as a 2D integral and this it valid if the lateral size of a QD is greater than the quantum-well width L.

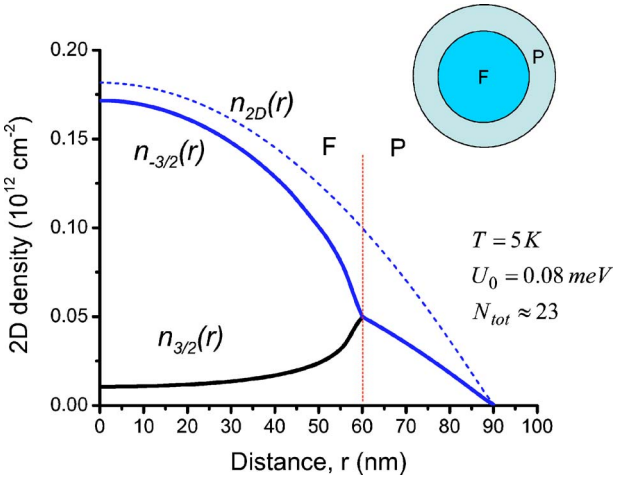

FIG. 2. (Color online) Calculated hole density as a function of the distance from the center of QD for a relatively small number of holes. The QD is divided into ferromagnetic (F) and paramagnetic phases (P). The dashed line represents the total 2D density. Inset: sketch of the QD structure.

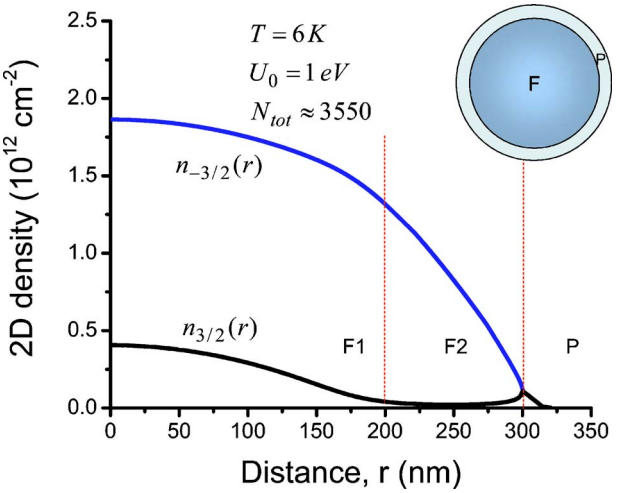

FIG. 3. (Color online) Calculated hole density as a function of the distance from the center of QD for a larger number of holes. The QD is divided into ferromagnetic ($F1$ and $F2$) and paramagnetic regions (P). Inset: schematics of the QD structure.

In the system with the top gates closely located to a quantum well, the 2D integral in the equation for $U_{\mathrm{Coul}}(\mathbf{r})$ is reduced to a linear function of n_{2D}[25] and is given by a local flat-capacitor formula

$$U_{\mathrm{Coul}}(\mathbf{r}) = \frac{4\pi e^2 d_1 n_{2D}(\mathbf{r})}{\epsilon_s}, \tag{9}$$

where d_1 is the distance between the QD plane and the top gate; the distance to the back metal contact is assumed to be larger, i.e., $d_2 \gg d_1$; ϵ_s is a dielectric constant of the semiconductor ($\epsilon_s = 12.5$). The approximation (9) has been successfully used in the past for description of several experiments on optical and electronic properties of modulated lateral structures.[26,27] By using the local approximation for the self-consistent potential (9), we reduce Eq. (8) to coupled nonlinear local equations which should be solved numerically. The total number of holes in a QD is determined by the chemical potential μ and the lateral-potential depth U_0. Electrostatics of the structure under study [Fig. 1(a)] is similar to that studied in Refs. 26–28 and we can use here the results of the above publications. If the barrier between the QD and back contact permits efficient tunneling, the chemical potential in the QD coincides with the potential of the back contact (i.e., $\mu = 0$). Simultaneously, the front barrier (usually made of AlGaAs) blocks tunneling between the QD and the top gate. Also, if $d_1 \ll d_2$, the potential U_0 becomes close to eV_1.

III. MAGNETIC PHASES IN QUANTUM DOTS

Figures 2–4 show numerical calculations for the local spin densities in a circular QD with $d_1 = 300$ Å, $\hbar\omega = 2$ meV, and $\mu = 0$; for the QD depth, we take $U_0 = -0.08$, -1, and -2 eV. A QD with the minimum free energy is circularly symmetric and can be split into different phases. The total number of holes in a QD is given by an integral $N_{\mathrm{tot,QD}} = \int n_{2D}(r) d^2\mathbf{r}$. The corresponding $N_{\mathrm{tot,QD}}$ for the above values of U_0 are estimated as 23, 3550, and 14 200. In QDs with relatively small $N_{\mathrm{tot,QD}}$ (Fig. 2), the system is split into ferromagnetic (F) and paramagnetic (P) phases. In Fig. 2, the carriers with spin $j_z = +3/2$ are pushed away from the center of QD, the total spin of holes is negative, and the Mn subsystem has a positive magnetization. This situation corresponds to the anti-ferromagnetic hole-Mn coupling ($\beta < 0$). With increasing the total number of carriers (Fig. 3), one can see the formation of another stripe within the ferromagnetic phase. This stripe is located between the center region of a QD and the paramagnetic phase and the holes in this stripe are almost fully spin-polarized. With further increasing $N_{\mathrm{tot,QD}}$ (Fig. 4) and for relatively low temperatures, the formation of the ferromagnetic stripe ($F2$) with fully-polarized holes becomes evident. Simultaneously, the paramagnetic

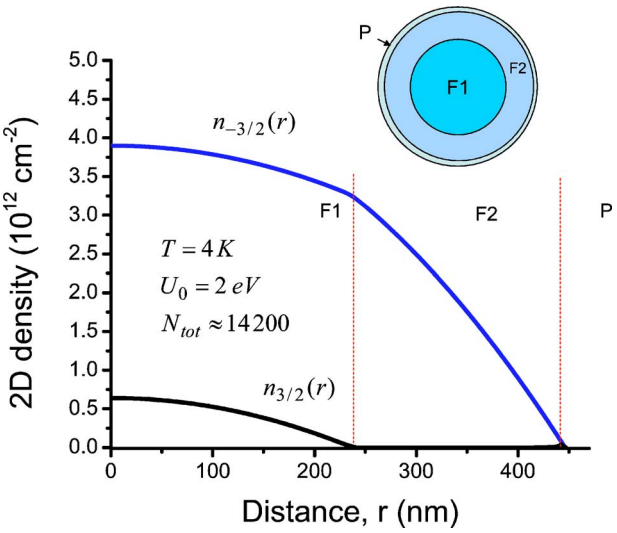

FIG. 4. (Color online) Calculated hole density as a function of the distance from the center of QD for a large number of holes at low temperature. The QD is divided into ferromagnetic ($F1$ and $F2$) and paramagnetic phases (P). Inset: schematics of the QD structure.

stripe becomes very narrow. Such a magnetic stricture of a QD can be understood by looking at the data in Fig. 1(b). At low temperatures, the function $N_{\rm spin}(N_{\rm 2D})$ becomes very close to the linear function $N_{\rm 2D}$ in an extended interval of $N_{\rm 2D}$. For example, at $T=4$ K, $N_{\rm spin}(N_{\rm 2D})\approx N_{\rm 2D}$ for $0.2\times10^{12}<N_{\rm 2D}<3\times10^{12}$. In the above interval of $N_{\rm 2D}$ at $T=4$ K, the hole subsystem is almost completely spin polarized.

It is interesting to estimate different types of energies contributing to the formation of stripes. It is easy to see that the Coulomb energy in Eqs. (8) dominates the ferromagnetic and single-particle (kinetic) energies. The Coulomb energy $U_{\rm Coul}=4\pi e^2 dN_{\rm 2D}/\epsilon_s\sim 90$ meV for $N_{\rm 2D}=2\times10^{11}$ cm^{-2} while the spin energy $|U^0_{\rm spin}|\sim 2$ meV for $N_{\rm spin}=2\times10^{11}$ cm^{-2} at $T=4$ K. The single-particle kinetic energy under the similar conditions $E_{\rm kin}\sim n_{\rm 2D}/D_{\rm 2D}\sim 1.2$ meV. For QDs with more carriers and higher $n_{\rm 2D}$, the above energies become increased but the condition $U_{\rm Coul}\gg|U^0_{\rm spin}|\sim E_{\rm kin}$ remains.

We can also obtain analytic solutions of Eqs. (8) under certain conditions. If both spin subsystems of holes ($j_z=\pm 3/2$) form a degenerate Fermi gas, the last term in Eqs. (8) becomes proportional to the Fermi energy $2n_{j_z}/D_{\rm 2D}$. Then, we can sum up the equations for $j_z=\pm 3/2$. The resulting equation does not contain the spin energy $U^0_{\rm spin}$ and can be solved analytically:

$$n_{\rm 2D}(r)=\frac{1}{4\pi e^2 d/\epsilon_s+\pi\hbar^2/m_{hh}}\left[|U_0|-\frac{m_{hh}\omega^2}{2}r^2\right]. \quad (10)$$

This formula can be applied, for example, to large QDs in the spatial region of the ferromagnetic phase $F1$, $0<r<R_{F1}$, where R_{F1} is the radius of the $F1$ phase (see Fig. 4). For this phase, spin densities can also be found analytically, by using the condition $n_{\rm spin}=n_{-3/2}-n_{+3/2}=-N_{\rm spin,saturation}$, where $N_{\rm spin,saturation}$ is a positive constant equal to $N_{\rm spin}$ at high $N_{\rm 2D}$ in Fig. 1(b); for $T=4$ K, $N_{\rm spin,saturation}=3.26\times10^{12}$ cm^{-2} [see Fig. 1(b)]. The formula (10) also describes the density distribution in the paramagnetic phase in the regions where the hole gas is degenerate ($E_f=n_{\rm 2D}/D_{\rm 2D}>k_BT$). For many other regimes, the spin densities should be found numerically. Since the Coulomb energy dominates the magnetic and kinetic terms, the total radius of a QD can be well estimated from Eq. (10) by putting $n_{\rm 2D}(R_{\rm QD})=0$. The resulting estimate $R_{\rm QD}\approx\sqrt{2|U_0|/[m_{hh}\omega^2]}$ is valid at low temperatures.

Experimentally, the stripe structure of a QD can be observed, for example, by spatially resolved optical spectroscopy.[29] In optical spectroscopy, a spatial resolution can be as small as 0.1 μm.[29] Simultaneously optical emission is sensitive to the spin-polarization of carriers. In an optical experiment, a ferromagnetic QD would be excited with weak nonpolarized illumination; the resulting local photoluminescence will be circularly polarized and reveal the formation of stripes with different magnetic structures.

Optical methods can also be used to write a magnetic state of QD (bit: "up"-"down"). This may be done with circularly polarized light. Polarized optical pumping can bring a QD into a required collective magnetic state with spins "up" or "down." In order to prepare a quantum dot in a required magnetic state, one can also use the magnetic field induced by an electric current driven through a metallic wire on the surface of a sample.

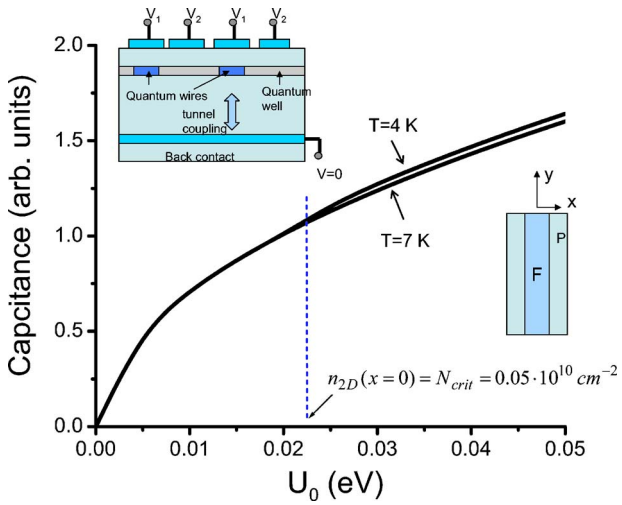

FIG. 5. (Color online) Calculated capacitance of a nanowire in the system with interdigitated metal gate (see inset on the left-hand side) for two temperatures 4 and 7 K. The inset on the right-hand side shows a top view of a nanowire with two phases.

Another method to observe the magnetic phases in nanostructures is the electrical-capacitance spectroscopy[27,28] which was successfully applied to observe, for example, compressible and incompressible stripes in electron quantum wires in the regime of the quantum Hall effect.[27,28] The capacitance spectroscopy has been also applied to lateral and self-assembled quantum dots (see, e.g., Ref. 11). For the nanostructures with relatively large sizes considered in this paper, the signature of the ferromagnetic phase in the capacitance spectra is expected to be relatively weak because of the inequality $U_{\rm Coul}\gg|U^0_{\rm spin}|$. However, the formation of the ferromagnetic phase can be recognized from a critical behavior of the capacitance spectrum as a function of temperature and voltage.

IV. CAPACITANCE SPECTROSCOPY AND MAGNETIC PHASES IN QUANTUM WIRES

As an example, we consider here quantum wires in a structure with the interdigitated metal gate (see inset in Fig. 5). In such a system, alternating voltages are applied to the metal strips located on the surface of a quantum well. Similar structures were studied experimentally in Ref. 27. We can calculate the capacitance of a wire as a derivative $C(V_1)=e(dN_{\rm tot,QW}/dV_1)l\approx e^2(dN_{\rm tot,QW}/dU_0)l$, where $N_{\rm tot,QW}$ is the linear density of carriers in a quantum wire and l is the length of a wire in the in-plane y direction. In the local approximation for the Coulomb potential [Eq. (9)], the problems of quantum dot and wire become similar. Figure 5 shows the capacitance of a quantum wire as a function of voltage for two temperatures, just below and above the Curie temperature $T_C=6.4$ K. One can see in Fig. 5 that at low temperatures ($T<T_C$) the capacitance becomes increased starting from a critical voltage $U_0/e\sim 0.02$ V. This voltage

corresponds to the minimum 2D density [$\sim 5\times 10^{10}$ cm^{-2} at $T=4$ K; see Fig. 1(b)] which is necessary to obtain the ferromagnetic phase stripe in the center of nanowire. Starting from this voltage, the central region of a nanowire contains a ferromagnetic stripe. The capacitance of a partially ferromagnetic wire becomes increased since the spin interaction makes a lateral potential well a little deeper and a wire can accommodate more carriers at a given voltage. If temperature increases just by 3 K, the ferromagnetic stripe vanishes and capacitance becomes reduced. This peculiar temperature behavior for $U_0 > 0.02$ eV can be taken as an evidence for the ferromagnetic phase.

V. CONCLUSIONS

In this paper, we studied quantum dots and wires with many interacting carriers within the quasiclassical approach. The strongest interaction in quantum dots with a relatively weak confinement and a large number of carriers comes from the Coulomb forces. However, a weaker ferromagnetic interaction determines the spin structure of a large quantum dot. Depending on the parameters, a quantum dot can be split into three phases.

ACKNOWLEDGMENTS

The author would like to thank Bruce McCombe for motivating discussions. This work was supported by Ohio University and the A.v. Humboldt Foundation.

[1] J. K. Furdyna, J. Appl. Phys. **65**, 29 (1988).
[2] *Semiconductor Spintronics and Quantum Computation*, edited by D. D. Awschalom, D. Loss, and N. Samarth (Springer-Verlag, Berlin, 2002); I. Zutic, J. Fabian, and S. Das Sarma, Rev. Mod. Phys. **76**, 323 (2004).
[3] C. Zener, Phys. Rev. **81**, 440 (1950); M. A. Ruderman and C. Kittel, *ibid.* **96**, 99 (1954).
[4] M. Abolfath, T. Jungwirth, J. Brum, and A. H. MacDonald, Phys. Rev. B **63**, 054418 (2001).
[5] T. Dietl and H. Ohno, Physica E (Amsterdam) **9**, 185 (2001).
[6] K. S. Burch, E. J. Singley, J. Stephens, R. K. Kawakami, D. D. Awschalom, and D. N. Basov, Phys. Rev. B **71**, 125340 (2005).
[7] A. D. Giddings, M. N. Khalid, T. Jungwirth, J. Wunderlich, S. Yasin, R. P. Campion, K. W. Edmonds, J. Sinova, K. Ito, K.-Y. Wang, D. Williams, B. L. Gallagher, and C. T. Foxon, Phys. Rev. Lett. **94**, 127202 (2005).
[8] C. Rüster, T. Borzenko, C. Gould, G. Schmidt, L. W. Molenkamp, X. Liu, T. J. Wojtowicz, J. K. Furdyna, Z. G. Yu, and M. E. Flatte, Phys. Rev. Lett. **91**, 216602 (2003).
[9] Y. D. Park, A. T. Hanbicki, S. C. Erwin, C. S. Hellberg, J. M. Sullivan, J. E. Mattson, T. F. Ambrose, A. Wilson, G. Spanos, and B. T. Jonker, Science **295**, 651 (2002); H. Ohno, D. Chiba, F. Matsukura, T. Omiya, E. Abe, T. Dietl, Y. Ohno, and K. Ohtani, Nature (London) **408**, 944 (2000).
[10] For the case of lithographically defined quantum dots, see, e.g., C. Sikorski and U. Merkt, Phys. Rev. Lett. **62**, 2164 (1989); D. Heitmann and J. P. Kotthaus, Phys. Today **46**, 56 (1993).
[11] For the case of self-assembled quantum dots, see, e.g., H. Drexler, D. Leonard, W. Hansen, J. P. Kotthaus, and P. M. Petroff, Phys. Rev. Lett. **73**, 2252 (1994); P. Schittenhelm, C. Engel, F. Findeis, G. Abstreiter, A. A. Darhuber, G. Bauer, A. O. Kosogov, and P. Werner, J. Vac. Sci. Technol. B **16**, 1575 (1998).
[12] A. K. Bhattacharjee and J. Perez-Conde, Phys. Rev. B **68**, 045303 (2003).
[13] A. O. Govorov, Phys. Rev. B **70**, 035321 (2004).
[14] A. O. Govorov and A. V. Kalameitsev, Phys. Rev. B **71**, 035338 (2005).
[15] J. I. Climente, M. Korkusinski, P. Hawrylak, and J. Planelles, Phys. Rev. B **71**, 125321 (2005).
[16] A. K. Bhattacharjee and C. Benoit a la Guillaume, Phys. Rev. B **55**, 10613 (1997).
[17] J. Fernandez-Rossier and L. Brey, Phys. Rev. Lett. **93**, 117201 (2004).
[18] Kai Chang, S. S. Li, J. B. Xia, and F. M. Peeters, Phys. Rev. B **69**, 235203 (2004).
[19] P. S. Dorozhkin, A. V. Chernenko, V. D. Kulakovskii, A. S. Brichkin, A. A. Maksimov, H. Schoemig, G. Bacher, A. Forchel, S. Lee, M. Dobrowolska, and J. K. Furdyna, Phys. Rev. B **68**, 195313 (2003).
[20] S. Mackowski, T. Gurung, T. A. Nguyen, H. E. Jackson, L. M. Smith, G. Karczewski, and J. Kossut, Appl. Phys. Lett. **84**, 3337 (2004).
[21] A. O. Govorov, Phys. Rev. B (to be published).
[22] X. Chen, M. Na, M. Cheon, S. Wang, H. Luo, B. D. McCombe, X. Liu, Y. Sasaki, T. Wojtowicz, J. K. Furdyna, S. J. Potashnik, and P. Schiffer, Appl. Phys. Lett. **81**, 511 (2002).
[23] J. Fernandez-Rossier and L. J. Sham, Phys. Rev. B **64**, 235323 (2001).
[24] T. Dietl, A. Haury, and Y. Merle d'Aubigne, Phys. Rev. B **55**, R3347 (1997).
[25] A. O. Govorov, V. M. Kovalev, and A. V. Chaplik, JETP Lett. **70**, 488 (1999).
[26] S. Zimmermann, A. O. Govorov, W. Hansen, J. P. Kotthaus, M. Bichler, and W. Wegscheider, Phys. Rev. B **56**, 13414 (1997).
[27] D. Schmerek, S. Manus, A. O. Govorov, W. Hansen, J. P. Kotthaus, and M. Holland, Phys. Rev. B **54**, 13816 (1996).
[28] A. O. Govorov, Phys. Rev. B **51**, 14498 (1995).
[29] H. D. Robinson, B. B. Goldberg, and J. L. Merz, Phys. Rev. B **64**, 075308 (2001).